*Inorg. Chem.* **2007**, *46*, 11017–11024


# Synthesis, Crystal Structure, and Magnetic Studies of Oxo-Centered Trinuclear Chromium(III) Complexes: $[Cr_3(\mu_3\text{-}O)(\mu_2\text{-}PhCOO)_6(H_2O)_3]NO_3\cdot 4H_2O\cdot 2CH_3OH$, a Case of Spin-Frustrated System, and $[Cr_3(\mu_3\text{-}O)(\mu_2\text{-}PhCOO)_2(\mu_2\text{-}OCH_2CH_3)_2(bpy)_2(NCS)_3]$, a New Type of $[Cr_3O]$ Core

**Albert Figuerola,[†] Vassilis Tangoulis,*[,‡] Joan Ribas,[†] Hans Hartl,[§] Irene Brüdgam,[§] Miguel Maestro,[⊥] and Carmen Diaz*[,†]**

*Departament de Química Inorgànica i Institut de Nanociència i Nanotecnologia, Universitat de Barcelona, Martí i Franquès, 1-11, 08028 Barcelona, Spain, Department of Chemistry, University of Patras, 26500 Patras, Greece, Department of Chemistry, Institut für Chemie, Anorganische und Analytische Chemie, Freie Universität Berlin, Berlin, Germany, and Departamento de Química Fundamental, Facultade de Ciencias, Universidade da Coruña, 15071 A Coruña, Spain*

Received March 30, 2007

The synthesis, crystal structure, and magnetic properties of two trinuclear oxo-centered carboxylate complexes are reported and discussed: $[Cr_3(\mu_3\text{-}O)(\mu_2\text{-}PhCOO)_6(H_2O)_3]NO_3\cdot 4H_2O\cdot 2CH_3OH$ (**1**) and $[Cr_3(\mu_3\text{-}O)(\mu_2\text{-}PhCOO)_2(\mu_2\text{-}OCH_2CH_3)_2(bpy)_2(NCS)_3]$ (**2**). For both complexes the crystal system is monoclinic, with space group *C*2/*c* for **1** and $P_1/n$ for **2**. The structure of complex **1** consists of discrete trinuclear cations, associated $NO_3^-$ anions, and lattice methanol and water molecules. The structure of complex **2** is built only by neutral discrete trinuclear entities. The most important feature of **2** is the unusual skeleton of the $[Cr_3O]$ core due to the lack of peripheral bridging ligands along one side of the triangular core, which is unique among the structurally characterized ($\mu_3$-oxo)-trichromium(III) complexes. Magnetic measurements were performed in the 2–300 K temperature range. For complex **1**, in the high-temperature region ($T > 8$ K), experimental data could be satisfactorily reproduced by using an isotropic exchange model, $H = -2J_{12}S_1S_2 - 2J_{13}S_1S_3 - 2J_{23}S_2S_3$ ($J_{12} = J_{13} = J_{23}$) with $J_{ij} = -10.1$ cm$^{-1}$, $g = 1.97$, and TIP $= 550 \times 10^{-6}$ emu mol$^{-1}$. The antisymmetric exchange interaction plays an important role in the magnetic behavior of the system, so in order to fit the experimental magnetic data at low temperature, a new magnetic model was used where this kind of interaction was also considered. The resulting fitting parameters are the following: $G_{zz} = 0.25$ cm$^{-1}$, $\delta = 2.5$ cm$^{-1}$, and TIP $= 550 \times 10^{-6}$ emu mol$^{-1}$. For complex **2**, the experimental data could be satisfactorily reproduced by using an isotropic exchange model, $H = -2J_1(S_1S_2 + S_1S_3) - 2J_2(S_2S_3)$ with $J_1 = -7.44$ cm$^{-1}$, $J_2 = -51.98$ cm$^{-1}$, and $g = 1.99$. The magnetization data allows us to deduce the ground term of $S = {}^1/_2$, characteristic of equilateral triangular chromium(III) for complex **1** and $S = {}^3/_2$ for complex **2**, which is confirmed by EPR measurements.

## Introduction

Trinuclear oxo-centered metal complexes of the general type $[M_3O(O_2CR)_6L_3]^{0/+}$,[1a] where L is water or pyridine and R is an alkyl or aryl group, have been of great interest as systems to test current theories of magnetic and electronic coupling between metal atoms. A feature that has attracted attention is that when the three metal atoms are identical, and of the same oxidation state, the complex nearly always fails to adopt the 3-fold symmetry that might be expected. One interesting phenomenon is spin frustration, which occurs when all the interactions between spin pairs cannot simultaneously have their optimal value. The simplest systems where this could be observed are an odd-member ring of antiferromagnetic coupled spins. In complexes which have the triangular $\mu_3$-oxo bridge $[M_3O]$ core, when all three

* To whom correspondence should be addressed. E-mail: carme.diaz@qi.ub.es (C.D.).
[†] Universitat de Barcelona.
[‡] University of Patras.
[§] Freie Universität Berlin.
[⊥] Universidade da Coruña.

(1) (a) Cannon, R. D.; White, R. P. *Prog. Inorg. Chem.* **1988**, *36*, 195. (b) Blake, A. B.; Yavari, A.; Hatfield, W. E.; Sethulekshmi, C. N. *J. Chem. Soc., Dalton Trans.* **1985**, 2509. (c) Vincent, J. B.; Chang, H. R.; Folting, K.; Huffman, J. C.; Christou, G.; Hendrickson, D. N. *J. Am. Chem. Soc.* **1987**, *109*, 5703.

10.1021/ic700606e CCC: $37.00 
Published on Web 11/16/2007

pairwise interactions are antiferromagnetic, there is the possibility of spin frustration if the three pairwise interactions are the same; then, only two of the three spin constraints can be satisfied simultaneously, and the system is geometrically frustrated. The ground state then is of intermediate spin, intermediate between the lowest and the highest spins possible for the three metal ions. It is well-established that the $\mu_3$-oxo bridge in $[M_3O(O_2CR)_6L_3]^{n+}$ complexes is dominant in propagating the exchange interaction.[1b,c] Oxo-centered trinuclear complexes of antiferromagnetic spins are quite common for transition metal ions like $Fe^{3+}$,[2] $Mn^{3+}$,[1c,3] and $Cr^{3+}$.[2k,4] The isotropic Hamiltonian for the interaction between any two spins can be written as the scalar product of the spin operators: $H = -\Sigma_{ij} J_{ij} S_i S_j$. Therefore, the energy is minimized for collinear parallel or antiparallel spin alignments. The available experimental data are in good agreement with the isotropic HDVV model in the region of relatively high temperatures. However, there are a number of serious discrepancies between the predictions of the theory and the experimental data at low temperatures. In order to interpret the magnetic properties of these frustrated systems, it is necessary to go beyond the framework of the above isotropic exchange model and to introduce an antisymmetric exchange interaction, $\mathbf{G}_{AB}$. This antisymmetric exchange interaction of the type

$$H_{AS} = \Sigma_{ij} \mathbf{G}_{ij} [S_i \times S_j]$$

where $\mathbf{G}_{ij} = -\mathbf{G}_{ij}$ is the antisymmetric vector constant. As was pointed out by Tsukerblat and co-workers,[5] this equation was introduced phenomenologically by Dzialoshinski to explain the weak ferromagnetism of $\alpha$-$Fe_2O_3$ and manganese carbonate crystals.[6] The microscopic meaning of the parameter **G** was revealed in the work of Moriya.[7] Therefore, the operator $H_{AS}$ is usually termed the Dzialoshinski−Moriya antisymmetric (AS) interaction. AS exchange leads to qualitative and quantitative changes in the temperature and field dependences of the magnetic susceptibility at low temperatures. These features are due to the nonlinear behavior of levels in the magnetic field when AS exchange is taken into account, and they consist of a reduction of the magnetic moments.[5] Information about $\mathbf{G}_{ij}$ values for isolated complexes is very scarce. The first experimental observation of the antisymmetric exchange parameter on the electronic properties of the trinuclear complex $[Cu_3(\mu_3\text{-OH})(\text{pyridine-2-aldoxime})_3(SO_4)]\cdot 10.5H_2O$ was made by Tsukerblat and co-workers.[8] Experimental applications of this exchange term have been reported for various $Cu^{2+}{}_3$ complexes[9,10] as well as for $Fe^{3+}{}_3$, and $Cr^{3+}{}_3$ carboxylates.[11,12]

In this work, we describe the synthesis, X-ray structure, and magnetic properties of two cyclic trimeric compounds: $[Cr_3(\mu_3\text{-O})(\mu_2\text{-PhCOO})_6(H_2O)_3]NO_3\cdot 4H_2O\cdot 2CH_3OH$ (**1**) and $[Cr_3(\mu_3\text{-O})(\mu_2\text{-PhCOO})_2(\mu_2\text{-OCH}_2\text{-CH}_3)_2(bpy)_2(NCS)_3]$ (**2**). Complex **1** shows a similar cationic structure to those already reported,[4k,m−4r] but the skeleton of the $[Cr_3O]$ core of complex **2** is unique among the structurally characterized ($\mu_3$-oxo)-trichromium(III) complexes.

The magnetic behavior of complex **1**, which can be regarded as a geometrically frustrated system, is studied by


(2) (a) Sowrey, F. E.; Tilford, C.; Wocadlo, S.; Anson, C. E.; Powell, A. K.; Bennington, S. M.; Montfrooij, W.; Jayasooriya, U. A.; Cannon, R. D. *J. Chem. Soc., Dalton Trans.* **2001**, 862. (b) Hibbs, W.; van Koningsbruggen, P. J.; Arif, A. M.; Shum, W. W.; Millar, J. S. *Inorg. Chem.* **2003**, *42*, 5645. (c) Boudalis, A. K.; Sanakis, Y.; Raptopoulou, C. P.; Terzis, A.; Tuchagues, J. P.; Perlepes, S. *Polyhedron* **2005**, *24*, 1540. (d) Zhang, K. L.; Shi, Y. J.; Gao, S.; Dai, Y. D.; Yu, K. B.; You, X. Z. *Inorg. Chem. Commun.* **2004**, *7*, 584. (e) Bing, Y.; Zhi-Da, C. *J. Coord. Chem.* **2002**, *55*, 241. (f) Supriya, S.; Latha, K. S.; Das, S. K. *Eur. J. Inorg. Chem.* **2005**, 357. (g) Supriya, S.; Manikumari, S.; Raghavaiah, P.; Das, S. K. *New J. Chem.* **2003**, *27*, 218. (h) Supriya, S.; Das, S. K. *New J. Chem.* **2003**, *27*, 1568. (i) Çelenligil-Çetin, R.; Staples, R. J.; Stavropoulos, P. *Inorg. Chem.* **2000**, *39*, 5838. (j) François, M.; Saleh, M. I.; Rabu, P.; Souhassou, M.; Malaman, B.; Steinmetz, J. *Solid State Sci.* **2005**, *7*, 1236. (k) Psycharis, V.; Raptopoulou, C. P.; Boudalis, A. K.; Sanakis, Y.; Fardis, M.; Diamantopoulos, G.; Papavassiliou, G. *Eur. J. Inorg. Chem.* **2006**, 3710. (l) Gorun, S. M.; Papaefthymiou, G. C.; Frankel, R. B.; Lippard, S. J. *J. Am. Chem. Soc.* **1987**, *109*, 4244−4255.

(3) (a) Li, J.; Yang, S.; Zhang, F.; Tang, Z.; Ma, S.; Shi, Q.; Wu, Q.; Huang, Z. *Inorg. Chim. Acta* **1999**, *294*, 109. (b) Cañada-Vilalta, C.; Huffman, J. C.; Streib, W. E.; Davidson, E. R.; Christou, G. *Polyhedron* **2001**, *20*, 1375. (c) Wu, R.; Poyraz, M.; Sowrey, F. E.; Anson, C. E.; Wocadlo, S.; Powell, A. K.; Jayasooriya, U. A.; Cannon, R. D.; Nakamoto, T.; Katada, M.; Sano, H. *Inorg. Chem.* **1998**, *37*, 1913.

(4) (a) Figgis, B. N.; Robertson, G. B. *Nature* **1965**, 694. (b) Schenk, K. J.; Güdel, H. U. *Inorg. Chem.* **1982**, *21*, 2253. (c) Gonzalez-Vergara, E.; Hegenauer, J.; Saltman, P.; Sabat, M.; Ibers, J. A. *Inorg. Chim. Acta* **1982**, *66*, 115. (d) Bradshaw, J. E.; Grossie, D. A.; Mullica, D. F.; Pennington, D. E. *Inorg. Chim. Acta* **1988**, *141*, 41. (e) Harton, A.; Nagi, M. K.; Glass, M. M.; Junk, P. C.; Atwood, J. L.; Voncent, J. B. *Inorg. Chim. Acta* **1994**, *217*, 171. (f) Anson, C. E.; Bourke, J. P.; Cannon, R. D.; Jayasooriya, U. A.; Molinier, M.; Powell, A. K. *Inorg. Chem.* **1997**, *36*, 1265. (g) Cannon, R. D.; Jayasooriya, U. A.; Sowrey, F. E.; Tilford, C.; Little, A.; Bouke, J. P.; Rogers, R. D.; Vicent, J. B.; Kearley, G. J. *Inorg. Chem.* **1998**, *37*, 5675. (h) Fujihara, T.; Aonahata, J.; Kumakura, S.; Nagasawa, A.; Murakami, K.; Ito, T. *Inorg. Chem.* **1998**, *37*, 3779. (i) Lieberman, R. L.; Bino, A.; Mirsky, N.; Summers, D. A.; Thompson, R. C. *Inorg. Chim. Acta* **2000**, *297*, 1. (j) Palii, S. P.; Richardson, D. E.; Hansen, M. L.; Iversen, B. B.; Larsen, F. K.; Singerean, L.; Timco, G. A.; Gerbeleu, N. V.; Jennings, K. R.; Eyler, J. R. *Inorg. Chim. Acta* **2001**, *319*, 23. (k) Vlachos, A.; Psycharis, V.; Raptopoulou, C. P.; Lalioti, N.; Sanakis, Y.; Diamantopoulos, G.; Fardis, M.; Karayanni, M.; Papavassiliou, G.; Terzis, A. *Inorg. Chim. Acta* **2004**, *357*, 3162. (l) Baranwal, B. P.; Fatma, T. *J. Mol. Struct.* **2005**, *750*, 72. (m) Winpenny, R.; Smith, A.; Coxall, B.; Parsons, S.; Messenger, D. Private communication, 2005. (n) Parsons, S.; Murrie, M.; Teat, S.; Winpenny, R.; Wood, P. Private communication, 2004. (o) Winpenny, R.; Smith, A.; Parsons, S.; Messenger, D. Private communication, 2005. (p) Winpenny, R.; Smith, A.; Parsons, S.; Messenger, D. Private communication, 2005. (q) Batsanov, A. S.; Struchkov, Y. T.; Gerbeleu, N. V.; Timko, G. A.; Manole, O. S. *Koord. Khim.* **1994**, *20*, 833. (r) Coxall, R. A.; Parkin, A.; Parsons, S.; Smith, A. A.; Timco, G. A.; Winpenny, R. *J. Solid State Chem.* **2001**, *159*, 321.

(5) Tsukerblat, B. S.; Belinskii, M. I.; Fainzil'berg, V. E. *Sov. Sci. Rev. B Chem.* **1987**, *9*, 337.

(6) Dzialoshinski, I. *Phys. Chem. Solids* **1958**, *4*, 241.

(7) (a) Moriya, T. *Phys Rev.* **1960**, *117*, 635. (b) Moriya, T. *Phys. Rev.* **1960**, *120*, 91.

(8) Tsukerblat, B. S.; Kuyavskaya, B. Y.; Belinskii, M. I.; Ablov, A. V. *Theor. Chim. Acta* **1975**, *38*, 131.

(9) (a) Yoon, J.; Mirica, L. M.; Stack, D. P.; Solomon, E. I. *J. Am. Chem. Soc.* **2004**, *126*, 12586. (b) Ferrer, S.; Lloret, F.; Bertomeu, I.; Alzuet, G.; Borrás, J.; García-Granda, S.; Liu-González, M.; Haasnot, J. G. *Inorg. Chem.* **2002**, *41*, 5821. (c) Ferrer, S.; Haasnot, J. G.; Reedijk, J.; Müller, E.; Biagini Cingi, M.; Lanfranchi, M.; Manotti Lanfredi, A. M.; Ribas, J. *Inorg. Chem.* **2000**, *39*, 1859. (d) Liu, X.; de Miranda, M. P.; McInnes, E. J. L.; Kilner, C. A.; Halcrow, M. A. *Dalton Trans.* **2004**, 59.

(10) (a) Padilla, J.; Gatteschi, D.; Chauduri, P. *Inorg. Chim. Acta* **1997**, *260*, 217. (b) Chauduri, P.; Karpenstein, I.; Winter, M.; Butzlaff, C.; Bill, E.; Trautwein, A. X.; Flörke, U.; Haupt, H. J. *J. Chem Soc., Chem. Commun.* **1992**, 321.

(11) Rakitin, Y. V.; Yablokov, Y. V.; Zelentsov, V. V. *J. Magn. Reson.* **1981**, *43*, 288.

(12) Nishimura, H.; Date, M. *J. Phys. Soc. Jpn.* **1985**, *54*, 395.

**Table 1.** Crystallographic Data for Complexes **1** and **2**

| | **1** | **2** |
|---|---|---|
| empirical formula | $C_{44}H_{58}Cr_3NO_{25}$ | $C_{41}H_{36}Cr_3N_7O_7S_3$ |
| formula mass | 1156.87 | 990.95 |
| cryst syst | monoclinic | monoclinic |
| space group | *C*2/c | $P_1/n$ |
| *Z* | 4 | 4 |
| *a* (Å) | 10.9596(9) | 12.037(3) |
| *b* (Å) | 24.9214(19) | 16.864(4) |
| *c* (Å) | 21.9436(17) | 21.384(5) |
| α (deg) | 90 | 90 |
| $\beta$ (deg) | 92.268(2) | 100.210(5) |
| $\gamma$ (deg) | 90 | 90 |
| *V* (Å$^3$) | 5988.7(8) | 4272.0(18) |
| $\rho$ (calcd) (g/cm$^3$) | 1.276 | 1.541 |
| $\mu_{calcd}$ (mm$^{-1}$) | 0.609 | 0.955 |
| $\lambda$(Mo Kα) (Å) | 0.71073 | 0.71073 |
| *T* (K) | 173(2) | 173(2) |
| $\theta$ range for data collection | 1.86−28.30° | 1.55−20.81° |
| total reflns | 18057 | 22149 |
| reflns $I > 2\sigma$ | 4420 | 3407 |
| reflexions collected | 7436 | 4473 |
| params refined | 359 | 644 |
| final *R* indices [$I > 2\sigma(I)$] | R1 = 0.0532 | R1 = 0.0507 |
| | wR2 = 0.1622 | wR2 = 0.1311 |
| final *R* indices [for all data] | R1 = 0.0904 | R1 = 0.0700 |
| | wR2 = 0.1809 | wR2 = 0.1433 |
| goodness-of-fit on $F^2$ | 0.991 | 1.035 |
| largest diff peak, hole (e Å$^{-3}$) | 1.255 −0.471 | 1.061 −0.472 |

considering that the antisymmetric exchange interaction is operating. The corresponding calculations and results are reported.

## Experimental Section

**Materials.** All starting materials were purchased from Aldrich and were used without further purification.

**Synthesis of the New Complexes. [$Cr_3(\mu_3$-O)($\mu_2$-PhCOO)$_6$-($H_2O)_3$]$NO_3\cdot 4H_2O\cdot 2CH_3OH$ (1).** A solution of $Cr(NO_3)_3\cdot 9H_2O$ (0.80 g, 2 mmol) in methanol (20 mL) was added to an acetonitrile (20 mL) solution of benzoic acid (1.45 g, 12 mmol) and stirred under reflux for 1 h. Green crystals, suitable for X-ray structure analysis, were grown by slow evaporation at room temperature of the green solution after 1 day (yields 90%). Anal. Calcd for **1** ($C_{44}H_{58}Cr_3NO_{25}$): C, 46.68; N, 1.21; H, 5.05. Found: C, 46.4; N, 1.2; H, 5.2.

**[$Cr_3(\mu_3$-O)($\mu_2$-PhCOO)$_2$($\mu_2$-OCH$_2$−CH$_3$)$_2$(bpy)$_2$(NCS)$_3$] (2).** A solution of $NH_4SCN$ (0.84 g, 10.98 mmol) in DMF (10 mL) and bpy (0.86 g, 5.49 mmol) were added to a solution of complex **1** (1.86 g, 1.83 mmol) in ethanol (15 mL). The resulting solution was allowed to stand at 138 °C for 1 day under autogenous pressure in a Teflon-lined stainless steel autoclave. Slow cooling of the resulting solution to room temperature afforded brown crystals suitable for X-ray structure analysis (yields 75%). Anal. Calcd for **2** ($C_{41}H_{36}Cr_3N_7O_7S_3$): C, 49.69; N, 9.89; H, 3.66; S, 9.71. Found: C, 50.0; N, 9.8; H, 3.7; S, 9.7.

**Crystal Structure Determination.** Crystal data and details on the data collection and refinement are summarized in Table 1. Suitable single crystals of **1** and **2** were selected and mounted on a Bruker SMART-CCD area diffractometer with graphite monochromated. Unit-cell parameters were determined from 359 frames for **1** and 244 for **2** of intensity data covering 0.3° in $\omega$ over a hemisphere of the reciprocal space by combination of three exposure sets, and refined by least-squares method. Intensities were collected using $\omega/2\theta$. Lorentz-polarization and absorption corrections were made.

**Table 2.** Selected Bond Lengths (Å) and Angles (deg) for **1**

| | | | |
|---|---|---|---|
| Cr1−O1 | 1.904(3) | Cr2−O2 | 1.957(2) |
| Cr1−O3 | 1.976(2) | Cr2−O4 | 1.968(2) |
| Cr1−O7 | 1.947(2) | Cr2−O6 | 1.973(3) |
| Cr1−O5 | 2.031(3) | Cr2−O8 | 1.974(3) |
| Cr2−O1 | 1.892(3) | Cr2−O9 | 2.049(2) |
| | | | |
| O1−Cr1−O7 | 95.64(7) | O4−Cr2−O6 | 169.34(10) |
| O7−Cr1−O7#1 | 168.73(13) | O1−Cr2−O8 | 95.60(9) |
| O1−Cr1−O3 | 93.44(7) | O2−Cr2−O8 | 170.42(10) |
| O7−Cr1−O3 | 87.69(11) | O4−Cr2−O8 | 86.54(11) |
| O7#1−Cr1−O3 | 91.63(11) | O6−Cr2−O8 | 89.02(12) |
| O3−Cr1−O3#1 | 173.12(14) | O1−Cr2−O9 | 177.97(11) |
| O1−Cr1−O5 | 180.0 | O2−Cr2−O9 | 84.80(10) |
| O7−Cr1−O5 | 84.36(7) | O4−Cr2−O9 | 84.05(11) |
| O3−Cr1−O5 | 86.56(7) | O6−Cr2−O9 | 85.97(11) |
| O1−Cr2−O2 | 93.81(8) | O8−Cr2−O9 | 85.84(11) |
| O1−Cr2−O4 | 94.60(8) | Cr2#1−O1−Cr2 | 120.01(14) |
| O2−Cr2−O4 | 94.48(10) | Cr2#1−O1−Cr1 | 120.00(7) |
| O1−Cr2−O6 | 95.47(9) | Cr2−O1−Cr1 | 120.00(7) |
| O2−Cr2−O6 | 88.31(11) | | |

The structures were solved by direct methods, using the SHELXS computer program,[13] and refined by full-matrix least-squares method with the SHELX97 computer program,[13] using 7436 reflections for **1** and 4473 reflections for **2**. The function minimized was $\Sigma w||F_o|^2 - |F_c|^2|^2$, where $w = [\sigma^2(I) + (0.1067P)^2]^{-1}$ for **1** and $w = [\sigma^2(I) + (0.0927P)^2 + 4.466P]^{-1}$ for **2**, and $P = (|F_o|^2 + 2|F_c|^2)/3$, $f$, $f'$, and $f''$ were taken from International Tables of X-ray Crystallography.[14] For **1**, the hydrogen atoms were calculated with the exception of those corresponding to the water and methanol molecules that could not be located. For **2**, 10 hydrogen atoms were calculated, and 25 hydrogen atoms were located from a difference synthesis, while the remaining hydrogen atoms were refined without constraints. The computed hydrogen atoms were refined using a riding model with the isotropic temperature factor for H atoms equal to 1.2 times the equivalent temperature factor of the atom which is linked.

**Physical Measurements.** Magnetic measurements were carried out in the "Unitat de Messures Magnètiques (Universitat de Barcelona)" on polycrystalline samples (20 mg) with a Quantum Design SQUID MPMS-XL magnetometer working in the 2−300 K range. The magnetic field was 10000G at high temperature and 200 G at low temperature. The field-dependent magnetization was measured in the applied magnetic field range 0−5 T at 2 K. The diamagnetic corrections were evaluated from Pascal's constants. The X-band EPR spectra were recorded on powder samples with a Bruker 300E automatic spectrometer, varying the temperature between 4 and 300 K.

## Results and Discussion

**Description of the Structure of Complexes [$Cr_3(\mu_3$-O)-($\mu_2$-PhCOO)$_6$($H_2O)_3$]$NO_3\cdot 4H_2O\cdot 2CH_3OH$ (1) and [$Cr_3(\mu_3$-O)($\mu_2$-PhCOO)$_2$($\mu_2$-OCH$_2$-CH$_3$)$_2$(bpy)$_2$(NCS)$_3$] (2).** The structure of these complexes was determined by X-ray crystallography. For both complexes, the crystal system is monoclinic, with space group *C*2/*c* for complex **1** and $P_1/n$ for complex **2**. Selected bond lengths and angles are listed in Tables 2 and 3 for complexes **1** and **2**, respectively.

The structure of complex **1** is built by trinuclear cations $[Cr_3(\mu_3\text{-O})(\mu_2\text{-PhCOO})_6(H_2O)_3]^+$, with $NO_3^-$ ions acting as

(13) Sheldrick, G. M. *A computer program for determination of crystal structure*; University of Göttingen: Göttingen, Germany, 1997.
(14) *International Tables of X-ray Crystallography*; Kynoch Press: Birmingham, U.K., 1974; Vol. iv, pp 99−100, 149.

**Table 3.** Selected Bond Lengths (Å) and Angles [deg] for **2**

| | | | |
|---|---|---|---|
| Cr01−O1 | 1.922(4) | Cr02−N2 | 2.019(6) |
| Cr01−O6 | 1.964(4) | Cr02−N21 | 2.064(5) |
| Cr01−O7 | 1.968(4) | Cr02−N22 | 2.076(5) |
| Cr01−O2 | 2.014(4) | Cr03−O1 | 1.902(4) |
| Cr01−O5 | 1.992(4) | Cr03−O7 | 1.958(4) |
| Cr01−N1 | 2.013(6) | Cr03−O4 | 1.988(4) |
| Cr02−O1 | 1.895(4) | Cr03−N3 | 2.015(6) |
| Cr02−O6 | 1.936(4) | Cr03−N32 | 2.050(5) |
| Cr02−O3 | 1.982(4) | Cr03−N31 | 2.064(5) |
| | | | |
| O1−Cr01−O6 | 80.38(16) | N22−Cr02−O1 | 95.21(17) |
| O1−Cr01−O7 | 82.00(15) | O6−Cr02−N22 | 175.88(19) |
| O6−Cr01−O7 | 162.14(17) | O3−Cr02−N22 | 91.04(19) |
| O1−Cr01−O5 | 90.93(16) | N2−Cr02−N22 | 87.9(2) |
| O5−Cr01−O6 | 87.87(17) | N22−Cr02−N21 | 78.1(2) |
| O5−Cr01−O7 | 89.55(16) | O1−Cr02−N21 | 91.96(17) |
| O1−Cr01−N1 | 176.90(19) | O1−Cr03−O7 | 82.77(16) |
| O6−Cr01−N1 | 101.7(2) | O1−Cr03−O4 | 90.40(16) |
| O7−Cr01−N1 | 96.03(19) | O4−Cr03−O7 | 93.62(16) |
| O5−Cr01−N1 | 91.45(19) | O1−Cr03−N3 | 177.70(18) |
| O1−Cr01−O2 | 89.24(16) | O7−Cr03−N3 | 94.96(18) |
| O6−Cr01−O2 | 91.12(17) | O4−Cr03−N3 | 90.10(18) |
| O7−Cr01−O2 | 91.52(16) | O1−Cr03−N32 | 90.11(17) |
| O5−Cr01−O2 | 178.93(18) | O7−Cr03−N32 | 93.58(17) |
| N1−Cr01−O2 | 88.42(19) | O4−Cr03−N32 | 172.78(18) |
| O1−Cr02−O6 | 81.76 (16) | N3−Cr03−N32 | 89.68(19) |
| O1−Cr02−O3 | 91.51(16) | O1−Cr03−N31 | 93.65(17) |
| O3−Cr02−O6 | 91.82(17) | O7−Cr03−N31 | 171.68(18) |
| N2−Cr02−O1 | 176.2(2) | O4−Cr03−N31 | 93.91(18) |
| O6−Cr02−N2 | 95.0(2) | N3−Cr03−N31 | 88.55(19) |
| O3−Cr02−N2 | 90.63(18) | N31−Cr03−N32 | 78.87(19) |
| O6−Cr02−N21 | 99.14(19) | Cr01−O1−Cr03 | 97.11(16) |
| O3−Cr02−N21 | 168.9(2) | Cr01−O1−Cr02 | 98.12(16) |
| N2−Cr02−N21 | 86.53(19) | Cr03−O1−Cr02 | 164.5(2) |

counteranion, and solvent methanol and water molecules. The ORTEP view, with atom labeling scheme and the core of the trinuclear entity are given in Figure 1a,b, respectively. Their skeletal structure is very similar to those of other trinuclear chromium(III) carboxylates.[4c,h,j,m−r,15−19] The three metal ions lie at the corners of a nearly equilateral triangle of separations: Cr2−Cr2 = 3.276 Å and Cr1−Cr2 = 3.287 Å. The center of the triangle is occupied by triply bridging oxygen not displaced out of the plane. The $\mu_3$-oxide atom is the common vertex of the coordination octahedral around the three $Cr^{3+}$ ions. The trigonal geometry at the $\mu_3$-O bridge is reflected by the analogous angles: Cr2−O1−Cr2 = 120.01° and Cr1−O1−Cr2 = 119.99°, very close to 120°. The benzoate ligand acts as bidentate and bridges couples of $Cr^{3+}$ ions, so that four benzoate oxygen atoms surround each chromium(III) ion. A water molecule, in trans position to the shared oxo ligand, acts as the sixth donor. Therefore, the coordination at each $Cr^{3+}$ ion includes six Cr−O bonds in a distorted octahedral environment. An examination of the angle values in the structure shows that all the $\mu_3$−O−Cr−O (benzoate) angles exceed 90°, whereas all the O(benzoate)−Cr−O(water) ones are smaller (Table 2). The trinuclear cations are self-assembled through hydrogen bonds

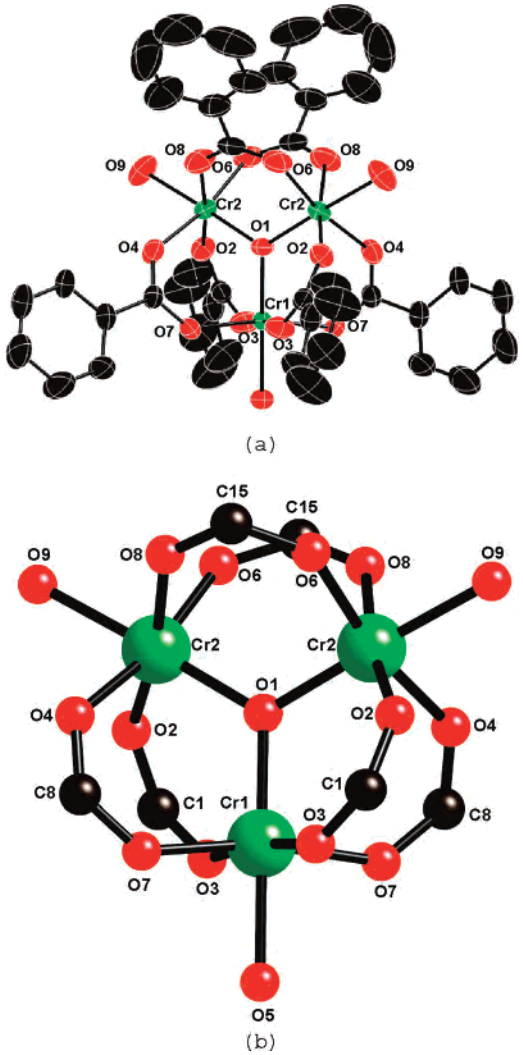


**Figure 1.** (a) ORTEP view of complex $[Cr_3(\mu_3\text{-}O)(\mu_2\text{-}PhCOO)_6(H_2O)_3]\text{-}NO_3\cdot 4H_2O\cdot 2CH_3OH$ (**1**) with atom labeling scheme. (b) Core of the trinuclear entity of **1**.

giving rise to a 2-D supramolecular structure in the *xy* plane (Figure S1, Supporting Information). The O9, O5 atoms of the water molecules coordinated to the chromium ions, and the O13/O13′ and O12 oxygen atoms of the $NO_3^-$ counteranion and the O18 of the methanol molecules of crystallization participated in this supramolecular structure. The shortest inter-trinuclear distance Cu−Cu is 8.15 Å. Short contact distances are shown in Table S1 (Supporting Information).

The structure of complex **2** is built only by neutral trinuclear $[Cr_3(\mu_3\text{-}O)(\mu_2\text{-}PhCOO)_2(\mu_2\text{-}OCH_2\text{-}CH_3)_2(bpy)_2\text{-}(NCS)_3]$ entities. The ORTEP view, with atom labeling scheme, and the core of the trinuclear entity are given in Figure 2a,b, respectively. The three metal atoms lie at the corners of a nearly isosceles triangle of separations Cr(01)···Cr(02) = 2.883 Å and Cr(01)···Cr(03) = 2.866 Å along equivalent sides of the isosceles triangle, and Cr(02)···Cr(03) = 3.768 Å along the inequivalent one. The center of the triangle is occupied by a triple-bridging oxygen atom. The equivalent Cr(01)−Cr(02) and Cr(01)−Cr(03) sides of the triangle are each bridged by the $\mu_2$-oxygen atom of the ethanolate ligand and by a bidentate benzoate group; no bridges were present along the inequivalent Cr(02)−Cr(03)

(15) Anson, C. E.; Chai-Sa'aed, N.; Bourke, J. P.; Cannon, R. D.; Jayasooriya, U. A.; Powell, A. K. *Inorg. Chem.* **1993**, *32*, 1502.
(16) Glowiak, T.; Kozlowsk, H.; Erre, L. S.; Micera, G. *Inorg. Chim. Acta* **1996**, *248*, 99.
(17) Mullica, D. F.; Pennington, D. E.; Bradshaw, J. E.; Sappenfield, E. L. *Inorg. Chim. Acta* **1992**, *191*, 3.
(18) Kato, H.; Nakata, K.; Nagasawa, A.; Yamaguchi, T.; Sasaki, Y.; Ito, T. *Bull. Chem. Soc. Jpn.* **1991**, *64*, 3463.
(19) Chang, S. C.; Jeffrey, G. A. *Acta Crystallogr.* **1970**, *B26*, 673.

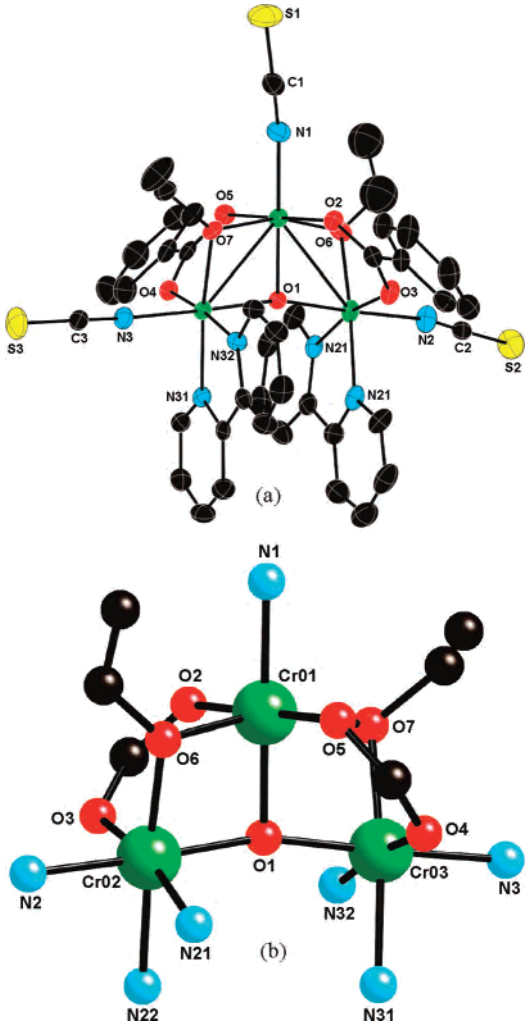


**Figure 2.** (a) ORTEP view of complex $[Cr_3(\mu_3\text{-}O)(\mu_2\text{-}PhCOO)_2(\mu_2\text{-}OCH_2CH_3)_2(bpy)_2(NCS)_3]$ (**2**) with atom labeling scheme. (b) Core of the trinuclear entity of **2**.

side. This lack of peripheral bridging ligands between Cr2−Cr3 is the most important structural feature which is unique among the structurally characterized ($\mu_3$-oxo)trichromium(III) complexes, and this characteristic is responsible for the anomalous Cr−O1−Cr: 98.12° (Cr(01)−O1−Cr(02)), 97.11° (Cr(01)−O1−Cr(03)), and 164.52° (Cr(02)−O−Cr(03). This indicates that the hybrids of the oxygen central atoms are farther than regular $sp^2$ hybridation. Chromium atoms Cr(02) and Cr(03) are also coordinated to bipyridine nitrogen atoms, and all three chromium atoms have a terminal thiocyanate ligand linked by the nitrogen atom. The Cr−O−Cr angles from the $\mu_2$-ethanolate are 95.30° (Cr(02)−O6−Cr(01)) and 93.79° (Cr(01)−O7−Cr(O3)). The neutral trinuclear entities are isolated; no hydrogen bonds or $\pi-\pi$ stacking are operating in the structure, so we can conclude that only van der Waals forces are responsible for the packing in the global structure.

**Magnetic Studies.$[Cr_3(\mu_3\text{-}O)(\mu_2\text{-}PhCOO)_6(H_2O)_3]NO_3\cdot 4H_2O\cdot 2CH_3OH$ (1).** The temperature dependence of the magnetic susceptibility data in $\chi_M T$ form ($\chi_M$ being the magnetic susceptibility per $[Cr_3]$ unit) is shown in Figure 3. The $\chi_M T$ data decrease smoothly from a value around 4.73 emu $mol^{-1}$ K at room temperature, smaller than the value

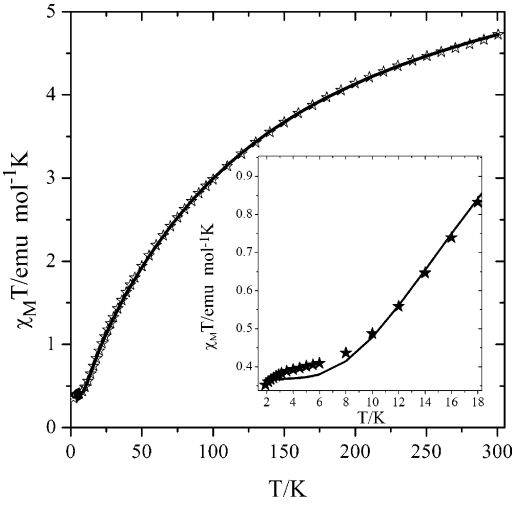


**Figure 3.** Magnetic susceptibility data in $\chi_M T$ form of **1**. Solid lines above the experimental data are theoretical curves derived from Hamiltonian 1. In the inset is shown the low-temperature susceptibility data along with the theoretical curve.

5.628 emu $mol^{-1}$ K expected for three independent $Cr^{3+}$ ions, to the value of 0.43 emu $mol^{-1}$ K at 10 K. Below that temperature, a plateaulike feature appears until 2 K (0.35 emu $mol^{-1}$ K) which is clear evidence that the total spin ($S_T$) for the ground state is $S_T = {}^1/_2$.

The isotropic Heisenberg Dirac van Vleck (HDvV) Hamiltonian (eq 1) is the main term used to interpret the magnetic data.

$$H = -2J_{12}S_1S_2 - 2J_{13}S_1S_3 - 2J_{23}S_2S_3 \qquad (1)$$

Superexchange has been studied in a large number of oxo-centered trinuclear complexes, and it is known that the coupling is antiferromagnetic ($J_{ij} < 0$). Since the three chromium atoms of the $[Cr_3O]$ unit define a quasiequilateral triangle, the three $Cr^{3+}$ ions can be considered equivalent, and so the three $J_{ij}$ constants are equal. If we assume three equal $J_{ij}$'s, the data are reasonably reproduced with $J_{ij} = -10.1$ $cm^{-1}$, $g = 1.97(1)$, and TIP $= 550 \times 10^{-6}$ emu $mol^{-1}$ (TIP = temperature-independent paramagnetism). The quality of the magnetic susceptibility data does not vary significantly if we adopt an isosceles triangle ($J_{12} = J_{13} \neq J_{23}$). The resolution of our data in the high-temperature range, however, does not allow us to make an accurate determination of the difference $|J_{12} - J_{23}|$. In the inset of Figure 3 is shown the low-temperature magnetic data where an obvious discrepancy exists between the magnetic model and the experimental points. In order to clarify the low-temperature behavior, a systematic measurement of the susceptibility data was carried out at different magnetic fields and is shown in Figure 4. It is well documented that the antisymmetric exchange interaction plays an important role in the magnetic behavior of the system, and so a new magnetic model was used where this kind of interaction was also considered:

$$H = -2J_0(S_1\cdot S_2 + S_2\cdot S_3) - 2J_1(S_1\cdot S_3) + G([S_1 \times S_2] + [S_2 \times S_3] + [S_3 \times S_1]) + (g_z \cos\theta + g_{xy}\sin\theta)\beta H(S_1 + S_2 + S_3) \qquad (2)$$

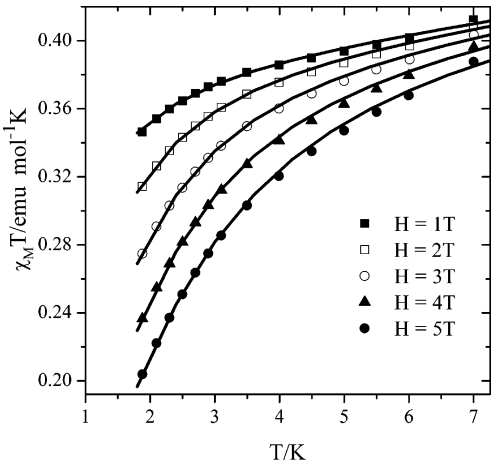


**Figure 4.** Low-temperature susceptibility data, at different magnetic fields, in the form of $\chi_M T$ vs $T$ of **1**. The solid lines represent the theoretical curves according to Hamiltonian 2. See text for details.

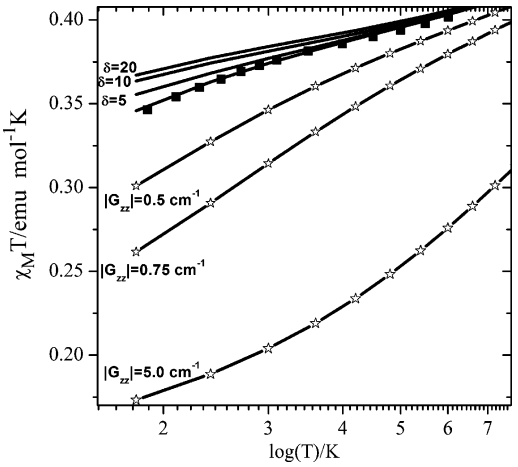


**Figure 5.** Simulation of the susceptibility equation in the form $\chi_M T$ vs log $T$ for different values of the **G** and $\delta$ parameters at external field $H$ = 1 T according to eq 2. Solid squares are the experimental points of the susceptibility data at $H$ = 1 T of **1**.

where $J_0$, $J_1$ are the isotropic exchange interactions (due to the symmetry lowering) and **G** is the antisymmetric exchange vector parameter for two-center interaction. In trigonal systems, the components of **G** are assumed to follow the relation $G_z \gg (G_x, G_y) \approx 0$ ($z$ being the 3-fold axis), which can be derived from the properties of the **G** vector.[7] This kind of interaction perturbs only the two lowest Kramers doublets of $S_T = {}^1/_2$, and the diagonalization yields the following energy levels:

$$E = \pm \frac{[\Delta E^2 + |M|^2 \pm 2\sqrt{\delta^2|M|^2 + |M\cdot G|^2}]^{1/2}}{2} \qquad (3)$$

where $|M| = \sqrt{(g_{xy}^2 \sin^2\theta + g_z^2 \cos^2\theta)}\ \beta H$ is the Zeeman term, $|G| = 4\sqrt{3}\,|G_{zz}|$, assuming $|G_{xx}| = |G_{yy}| \sim 0$ which is valid for a weakly axial system with $J_0 \approx J_1$, $|M\cdot G| = 4\sqrt{3}\, G_{zz} g_z \beta H \cos\theta$, and $\Delta E = \sqrt{\delta^2 + |G|^2}$ while the $\delta$ factor is equal to $4|J_0 - J_1|$. It must be pointed out that the sign of the **G** is also undefined under these conditions. It has been shown that $S_T = {}^3/_2$ is not perturbed by the antisymmetric exchange term, **G**, and does not affect the description of the $S_T = {}^1/_2$ states.

The components of the susceptibility tensor were calculated according to a generalized susceptibility equation,[8] and it was necessary to consider the parallel and perpendicular susceptibility components separately, since they are affected differently by the **G** vector. Using this approach, it was possible to fit the low-temperature data, 1.8−8 K, and the fitting results are shown in Figure 4 as solid lines while the resulting fitting parameters are, assuming $g_{xy} = g_z = 2.0$ as fixed, $|G_{zz}| = 0.25$ cm$^{-1}$, $\delta = 2.5$ cm$^{-1}$, TIP $= 550 \times 10^{-6}$ emu mol$^{-1}$. In order to investigate the influence of **G** and $\delta$ parameters in the low-temperature behavior of the susceptibility, different simulations were carried out and are shown in Figure 5. While each of the two paramaters varied, the other one was fixed to the value obtained from the fitting procedure. When the $\delta$ factor increases, the susceptibility plateaus are shifted toward higher values (closer to 0.375 emu mol$^{-1}$ K) while an increase in the **G** parameter causes a drastic divergence from the plateau to appear. In Figure S2 (Supporting Information) is shown a simulation where only the Zeeman part of eq 1 was considered fixing (**G**, $\delta$) = (0, 0). As it is clearly shown, a more anisotropic Hamiltonian is necessary.

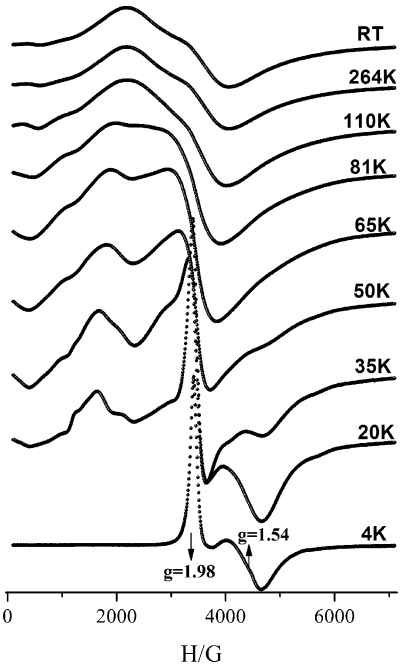


**Figure 6.** EPR spectra from a polycrystalline sample of **1** recorded at different temperatures from 4 K to room temperature. Other EPR conditions: modulation amplitude, 10 $G_{pp}$; microwave frequency, 9.40 GHz.

Magnetization data in the field range 0−6.5 T at 2 K are shown in Figure S3 (Supporting Information) along with the Brillouin function of a $S_T = {}^1/_2$ system with $g = 2$. This behavior is in accordance with the susceptibility data and reveals that the ground state is indeed an $S_T = {}^1/_2$ one. It was very difficult to extract information about the previous parameters from the magnetization data.

**EPR Spectroscopy.** EPR spectra from a polycrystalline sample of complex **1** at different temperatures from 4 K to room temperature are shown in Figure 6. At 4.2 K a strong absorption peak is observed at $g_{eff} = 1.97$ accompanied by a derivative feature at $g_{eff} = 1.70$. We attribute these signals

to an $S = {}^1/_2$ with axial **g**-tensors ($g_{||}$, $g_\perp$) = (1.98, 1.54). The temperature dependence of these signals indicates that their origin is from the ground state since after 20 K new signals appear at lower magnetic fields revealing the population of excited states.

For exchange coupled trimers, the large anisotropy in the **g**-tensor for the $S = {}^1/_2$ ground state with a rather small $g_\perp$ value is usually attributed to the effects of an antisymmetric exchange interaction according to eq 2.[20−22] The effect of this antisymmetric interaction is to induce an axial anisotropy in the **g**-tensor. More explicitly, the $g_{||}$ component is not affected whereas a shift toward lower **g**-values is observed for the $g_\perp$ component. From the EPR findings, compound **1** has isosceles magnetic symmetry or lower ($\delta \neq 0$); the antisymmetric exchange is important ($\mathbf{G} \neq 0$), and $\Delta E > h\nu$. The resulting relationship is[11]

$$g_\perp = g_0\left[\frac{\delta^2 - (h\nu)^2}{\Delta E^2 - (h\nu)^2}\right]^{1/2} \quad (4)$$

where $h\nu$ is the microwave energy ($\approx$0.31 cm$^{-1}$), $g_0$ is the true $g$ calculated from the magnetic studies ($g_{xy} = g_z = 2.0$), and all the other symbols have the meaning defined in eq 2. According to the fitting results of the susceptibility data, $g_\perp/g_0 = 0.78$, which is close to the value obtained from the EPR spectrum (0.77). This is clear evidence that the susceptibility results are in accordance with the EPR findings.

**$[Cr_3(\mu_3\text{-}O)(\mu_2\text{-}PhCOO)_2(\mu_2\text{-}OCH_2{-}CH_3)_2(bpy)_2(NCS)_3]$ (2).** The temperature dependence of the magnetic susceptibility data in the $\chi_M T$ form ($\chi_M$ being the magnetic susceptibility per [$Cr_3$] entity) is shown in Figure 7, top. At room temperature, the $\chi_M T$ value is 3.29 emu mol$^{-1}$ K, smaller than the value of 5.628 emu mol$^{-1}$ K expected for three independent $Cr^{3+}$ ions, and decreases to the value of 1.88 emu mol$^{-1}$ K at 50 K. After that temperature, a plateau appears until 2 K, which is clear evidence that the total spin ($S_T$) for the ground state is equal to ${}^3/_2$. The fit of the experimental data, corrected for diamagnetic contributions and TIP ($240 \times 10^{-6}$/$Cr^{3+}$),[23] was performed according with the isotropic HDvV Hamiltonian (eq 5)

$$H = -2J_1(S_1S_2 + S_1S_3) - 2J_2(S_2S_3) \quad (5)$$

where $J_1$ corresponds to the coupling through the equivalent sides of the triangle and $J_2$ corresponds to the nonequivalent one (Figure 7, top). The free parameters were $J_1$, $J_2$, and $g$. The fit made by the irreducible tensor operator formalism (ITO), using CLUMAG program,[24] gave the following results: $J_1 = -7.44$ cm$^{-1}$, $J_2 = -51.98$ cm$^{-1}$, $g = 1.99$ and $R = 2.67 \times 10^{-4}$.

Magnetization data in the field range 0−5 T at 2 K is shown in Figure 7 (bottom) along with the Brillouin function

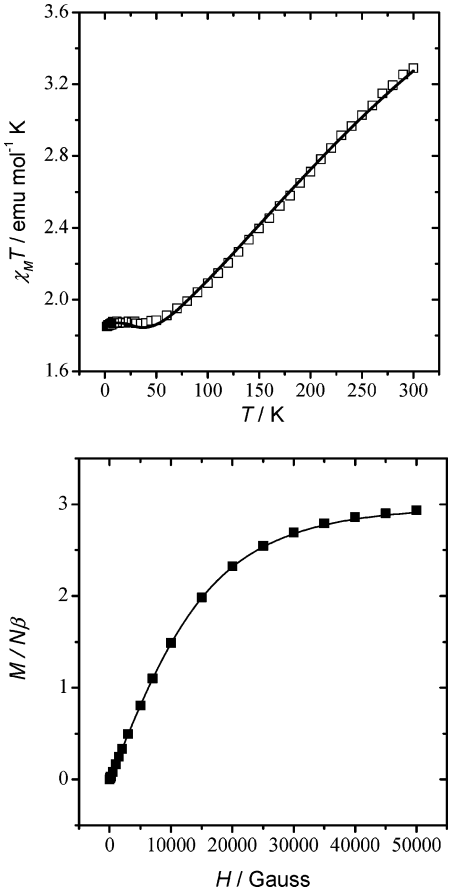


**Figure 7.** Top: Thermal dependence at 10000 G of $\chi_M T$ of **2**. Bottom: Magnetization vs $H$ (2 K) of **2**.

of a $S_T = {}^3/_2$ system with $g = 1.99$. This behavior is in accordance with the susceptibility data.

**EPR Spectroscopy.** X-band EPR measurements were carried out in powder samples of **2** and are shown in Figure S4 (Supporting Information). In the powder spectrum at 4 K, there are well-resolved peaks (shown with asterisks in Figure 8), which appear to belong to excited states such as the narrow small peak at about $g = 4.5$ as well as the well defined shoulder at $g = 3.14$. Also, for fields greater than 5000 G, it is difficult to observe the contribution of excited states. All these transitions were excluded from the simulation procedure that was carried out with the following Hamiltonian equation for a spin $S = {}^3/_2$:[25]

$$H = D\left[S_z^2 - \frac{1}{3}S(S+1)\right] + E(S_x^2 - S_y^2) + g_z\mu_B H_z S_z + g_x\mu_B H_x S_x + g_y\mu_B H_y S_y$$

The simulated spectrum is also shown in Figure 8 as a solid line.

An isotropic magnetic-field domain line width was used for the powder spectrum (lw = 35 G), while the broadness of the spectrum reveals the $g$-strain effects. Gaussian distributions of the $g$-principal values were used, and the results are ($\sigma g_x = \sigma g_y = 0.1$, $\sigma g_z = 0.2$). The principal $g$-values for the powder spectrum are $g_{xy} = 1.96(1)$, $g_z =$

(20) Bencini, A.; Gatteschi, D. In *EPR of Exchange Coupled Systems*; Springer-Verlag: New York, 1990.
(21) Gaponenko, V. A.; Eremin, M. V.; Yablokov, Y. V. *Sov. Phys. Solid State* **1973**, *15*, 909.
(22) Honda, M.; Morita, M.; Date, M. *J. Phys. Soc. Jpn.* **1992**, *61*, 3773.
(23) Boca, R. *Struct. Bonding* **2006**, *117*, 105.
(24) Gatteschi, D.; Pardi, L. *Gazz. Chim. Ital.* **1993**, *123*, 231.
(25) Stoll, S. Spectral Simulations in Solid-State EPR. Ph.D. Thesis, ETH Zurich, 2003.

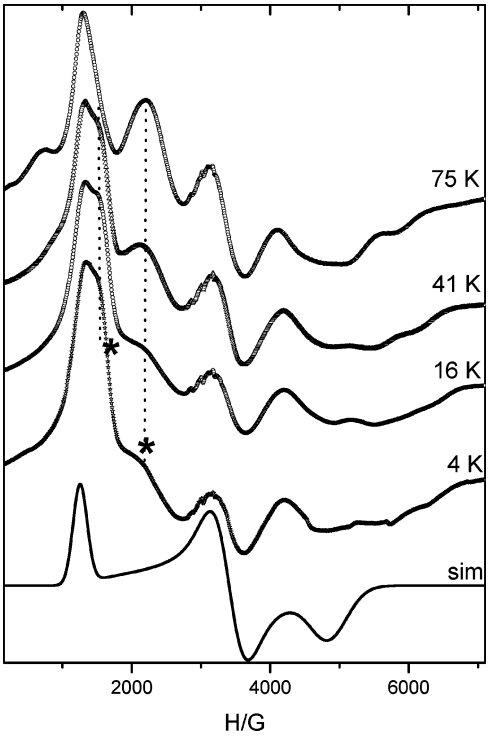


**Figure 8.** Simulated EPR spectrum (sim line) and temperature dependence of the powder spectra showing with asterisks transitions belonging to excited states. See text for details.

1.98(1). The values for the crystal field terms are $D = 1.5$-(5) $cm^{-1}$ and $\lambda = E/D = 0.3$, revealing the rhombic character of the system. Gaussian distributions of the $D$ and $E$ parameters were also used ($\sigma(D) = 0.3$, $\sigma(E) = 0.03$). Several complexes of $Cr^{3+}$ have large $D$-values and were calculated through simulations of EPR X-band spectra.[26] The simulation showed that the experimental line shape cannot be reproduced by an $S = {}^3/_2$ system with a well-defined value for $E/D$, even if one employs angular dependent line shape distributions of the type $W^2 = \sqrt{\sum W_i^2 l_i^2}$, where $l_i$ denotes the direction cosines of the applied field. There are well-resolved peaks which appear to belong to excited states and influence the line shape dramatically.

## Conclusions

The kinetically inert nature of the $Cr^{3+}$ ion usually requires reactions to be carried out at high temperature to obtain polymetallic clusters of high nuclearity:[27] one of the most successful synthetic routes has involved the direct heating of basic carboxylates $[Cr_3O(O_2CR)_6(H_3O)_3]^+$. The hydrothermal reaction of complex **1** in ethanol, $SCN^-$, and bpy produces complex **2** which involves loss of the three coordinated water molecules and four carboxylic acids and the coordination of three thiocyanate ions, three ethoxo bridging ligands, and two bpy molecules. A cluster of higher nuclearity has not been obtained, but a new skeleton of the $[Cr_3O]$ core was found.

In order to justify the low-temperature magnetic behavior of complex **1**, the antisymmetric exchange interaction term (**G**) was added to the HDvV Hamiltonian which represents the spin−orbit coupling attributed to the orbitally degenerated ground term. This antisymmetric term splits the two $S = {}^1/_2$ Kramers doublets and introduces an axial anisotropy in the system which can be clearly observed by EPR spectroscopy: The $g_{||}$ and $g_\perp$ values are 1.98 and 1.54, respectively, at 2 K. The magnitude of the $J$ value is similar to the value of the interaction constant observed in analogous $[Cr_3O]$ complexes previously reported.

Complex **2** shows different geometry, and one of the interactions between two chromium(III) ions ($J_2$) is different from the other two ($J_1$). The $J_1$ value includes the coupling through the triple-bridging oxygen atom, the benzoate, and the ethanolate bridging ligands. The magnitude of $J_2$ is the highest, since the interaction is mediated by an oxo bridged with a CrOCr angle of 164.5° for which a high value of about $-60$ $cm^{-1}$ is expected for the exchange coupling constant by the literature.[28] The magnetization data allows us to deduce the ground term of $S = {}^1/_2$, characteristic of equilateral triangular chromium(III), for complex **1** and $S = {}^3/_2$ for complex **2**, which is confirmed by EPR measurements.

**Acknowledgment.** This work was financially supported by the Spanish Government (Grant CTQ2006-03949). We also thank Núria Clos, Unitat de Messures Magnètiques, Serveis Científics i Tècnics, Universitat de Barcelona, for the magnetic measurements.

**Supporting Information Available:** Additional tables and figures. CIF data. CCDC-634867−634868 (**1** and **2**), which can be obtained free of charge from the Cambridge Crystallographic Data Centre via www.ccdc.cam.ac.uk/data_request/cif. This material is available free of charge via the Internet at http://pubs.acs.org.

IC700606E

(26) Shaham, N.; Cohen, H.; Meyerstein, D.; Bill, E. *J. Chem. Soc., Dalton Trans.* **2000**, 3082 and references therein.

(27) (a) Talbot-Eeckelaers, C. E.; Rajaraman, G.; Cano, J.; Aromí, G.; Ruiz, E.; Brechin, E. K. *Eur. J. Inorg. Chem.* **2006**, 3382. (b) Laye, R. H.; McInnes, E. J. L. *Eur. J. Inorg. Chem.* **2004**, 2811. (c) McInnes, E. J. L.; Piligkos, S.; Timco, G. A.; Winpenny, R. E. P. *Coord. Chem. Rev.* **2005**, *249*, 2577. (d) Bino, A.; Johnston, D. C.; Goshorn, D. P.; Halberd, T. R.; Stiefel, E. I. *Science* **1988**, *241*, 1479.

(28) Wang, C.; Fink, K.; Staemmler, V. *Chem. Phys.* **1995**, *201*, 87.